Cell Reports

Report

Cold-Induced Browning of Inguinal White Adipose Tissue Is Independent of Adipose Tissue Cyclooxygenase-2

Graphical Abstract

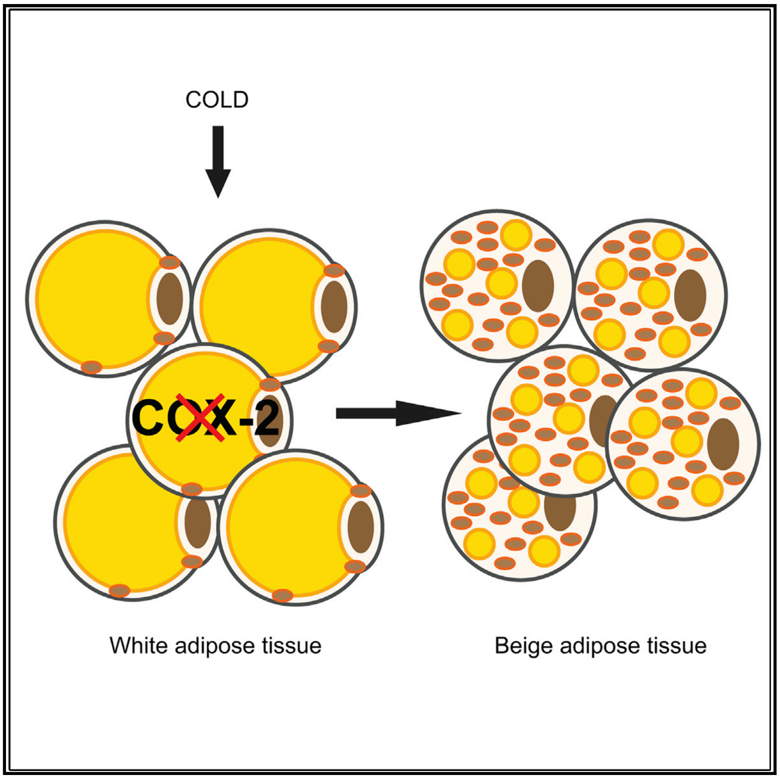

Highlights

- COX-2 is undetectable in inguinal adipose tissue by spectrometry and immunoblotting
- Cold exposure does not upregulate COX-2 expression in inguinal white adipose tissue
- COX-2 is not required for cold-induced browning of inguinal white adipose tissue

Authors

Georgios K. Paschos, Soon Yew Tang, Katherine N. Theken, ..., Weili Yan, John Lawson, Garret A. FitzGerald

Correspondence

garret@upenn.edu

In Brief

COX-2 is of importance during development. Browning of inguinal white adipose tissue is involved in metabolic health and reduced susceptibility to obesity. This study tested the involvement of COX-2 in browning of inguinal white adipose tissue and found no role for COX-2.

Paschos et al., 2018, Cell Reports *24*, 809–814
July 24, 2018 © 2018 The Authors.
https://doi.org/10.1016/j.celrep.2018.06.082

OPEN ACCESS
CellPress

Cold-Induced Browning of Inguinal White Adipose Tissue Is Independent of Adipose Tissue Cyclooxygenase-2

Georgios K. Paschos,[1,3] Soon Yew Tang,[1,3] Katherine N. Theken,[1] Xuanwen Li,[1] Ioannis Verginadis,[2] Damien Lekkas,[1] Lindsay Herman,[1] Weili Yan,[1] John Lawson,[1] and Garret A. FitzGerald[1,4,*]
[1]Institute for Translational Medicine and Therapeutics, Perelman School of Medicine, University of Pennsylvania, Philadelphia, PA 19104-5127, USA
[2]Department of Radiation Oncology, Perelman School of Medicine, University of Pennsylvania, Philadelphia, PA 19104-5127, USA
[3]These authors contributed equally
[4]Lead Contact
*Correspondence: garret@upenn.edu
https://doi.org/10.1016/j.celrep.2018.06.082

SUMMARY

Previous studies using genetic mouse models have implicated COX-2 in the browning of white adipose tissues (WATs) in mice during cold exposure. However, COX-2 is important during development, and conventional knockouts (KOs) exhibit many defects, conditioned by genetic background. Similarly, the physiological relevance of transgenic overexpression of COX-2 is questionable. In the present study, we utilized mice in which COX-2 was deleted postnatally, bypassing the consequences of enzyme deficiency during development. Despite activation of thermogenesis and browning of inguinal WAT, cold exposure failed to increase COX-2 expression in the adipose tissues of mice with different genetic backgrounds, and the body temperature response to cold was unaltered in postnatal global COX-2 KOs. Selective disruption of COX-2 in adipose tissues also failed detectably to impact systemic prostaglandin biosynthesis. Browning of inguinal WATs induced by exposure to cold is independent of adipose tissue COX-2.

INTRODUCTION

Cyclooxygenase-2 (COX-2) is a rate-limiting enzyme in the conversion of arachidonic acid to prostaglandins (Smith, 1992). It has been reported previously that COX-2 plays an important role in the formation of beige/brite fat in white adipose tissue (WAT) depots in mice on cold exposure. These studies have been based on the use of both genetic manipulations and pharmacological tools (Madsen et al., 2010; Vegiopoulos et al., 2010). However, there have been notable limitations to these approaches. For example, the selectivity of inhibition of COX-2 *in vivo* was not established in the case of the pharmacological experiments, while the two genetic models of manipulation of COX-2 expression—conventional global deletion of the enzyme and transgenic overexpression in skin cells—have distinct limitations. For example, COX-2 plays many important roles in development (Morham et al., 1995) and conventional knockouts (KOs) exhibit a range of defects, including age-dependent expression of myocardial fibrosis and renal insufficiency. In the case of mice overexpressing COX-2 in skin, there is thinning of body hair (Neufang et al., 2001), which would lead to the activation of thermogenesis due to increased heat loss at normal housing temperature (Nedergaard and Cannon, 2014). Additionally, prostaglandin products of COX-2 are formed in trace amounts and act as autacoids; thus, it is always difficult to know the physiological relevance of a system in which product formation is increased by orders of magnitude. Here, we used mice in which global COX-2 deletion was achieved postnatally by a tamoxifen-inducible form of Cre recombinase, bypassing the importance of COX-2 deficiency during development (Wang et al., 2009; Yu et al., 2012). Finally, we combined physiological assessment of transgenic mice having global and adipocyte-specific deletions of COX-2 with quantitative assessment of product formation using mass spectrometry.

RESULTS AND DISCUSSION

Cold Does Not Upregulate COX-2 or COX-1 in Either White or Brown Adipose Tissues

We first tested the effect of exposure to cold on COX-2 expression in adipose tissues, including inguinal WAT (iWAT), gonadal WAT (gWAT), and interscapular brown adipose tissue (iBAT). COX-2 was undetectable by western blotting in adipose tissue from mice maintained at 28°C (Figure 1A; Figure S1A). Contrary to previous reports (Madsen et al., 2010; Vegiopoulos et al., 2010), we found no increase in COX-2 after wild-type mice were exposed to cold for 6 days (Figure 1A; Figure S1A). We confirmed this by measuring COX-2 protein, using either western blotting or mass spectrometry in adipose tissue after cold exposure for 6 days. Despite the sensitivity of detection by mass spectrometry, we were unable to detect COX-2 protein (Figure S1C). COX-1 was detected in iWAT, gWAT, and iBAT from mice maintained at 28°C but, similar to COX-2, COX-1 levels did not increase after exposure of the mice to cold for 6 days (Figure 1B; Figures S1B and S1D). *Cox-2* and *Cox-1* gene expression did not increase in adipose tissues either

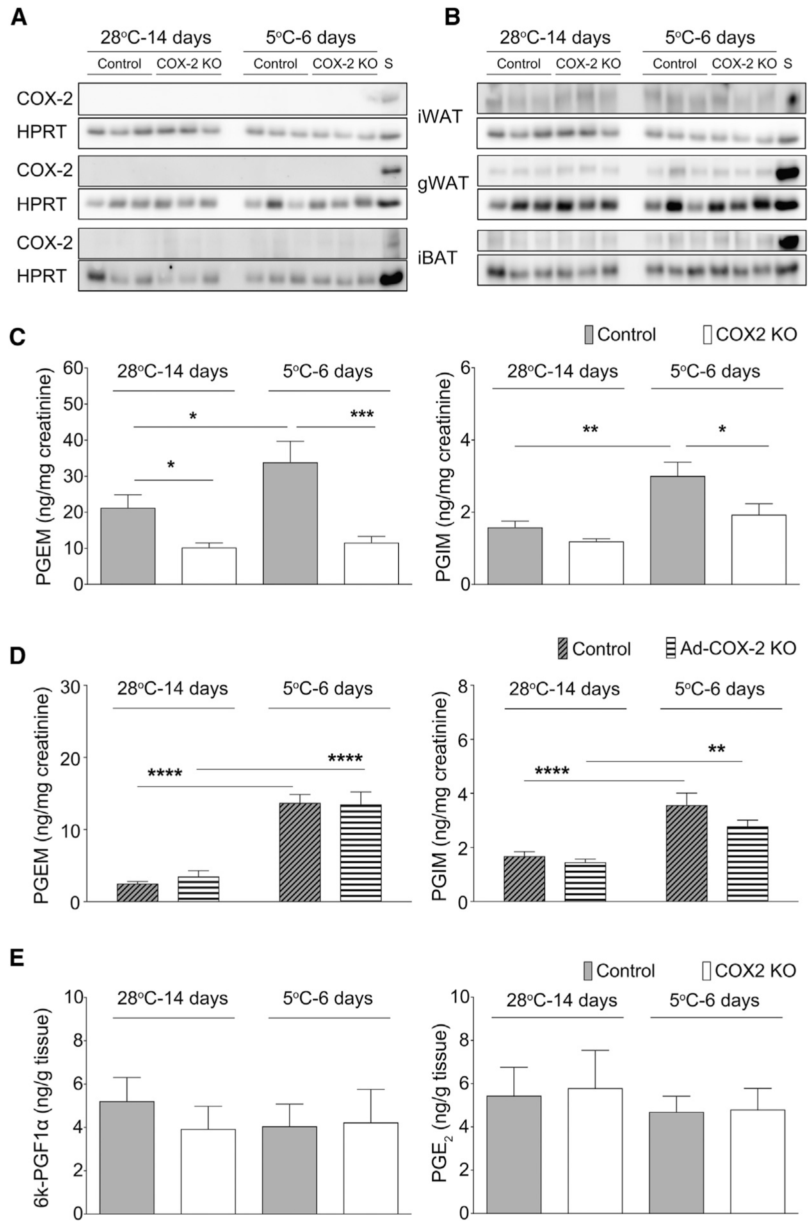

Figure 1. Cold Exposure Fails to Upregulate COX-2 and COX-1 Expression in Adipose Tissues

(A and B) COX-2 (A) and COX-1 (B) protein levels were examined by immunoblotting in inguinal white adipose tissue (iWAT), gonadal white adipose tissue (gWAT), and interscapular brown adipose tissue (iBAT) from mice housed at 28°C and 5°C. In (A), COX-2 was not detected in adipose tissues, regardless of genotypes and housing temperatures. HPRT was used as a loading control. Representative images of 6–8 independent experiments are shown. S-spleen was used as positive control.

(C) Urine samples from mice housed at 28°C and 5°C were analyzed for prostanoid metabolites by liquid chromatography-mass spectrometry as described in the Supplemental Experimental Procedures. Urinary 7-hydroxy-5,11-diketotetranorprostane-1,16-dioic acid (PGEM) and 2,3-dinor 6-keto $PGF_{1\alpha}$ (PGIM) were increased in control mice housed at 5°C for 6 days compared with mice housed at 28°C. Global COX-2 deletion depressed urinary PGEM and PGIM. A two-way ANOVA showed a significant effect of cold exposure and genotype on urinary PGEM and PGIM. Genotype, temperature, and interaction: for PGEM, $p < 0.0001$, $p = 0.0445$, and $p = 0.1008$; and for PGIM, $p = 0.0076$, $p = 0.0002$, and $p = 0.1879$. Holm-Sidak's multiple comparison tests were used to test significant differences between controls and COX-2 mutants at 28°C and 5°C. Data are expressed as mean ± SEM. *$p < 0.05$, **$p < 0.01$, ***$p < 0.001$, ****$p < 0.0001$; n = 9–11.

(D) Disruption of COX-2 in adipocytes (Ad-COX-2 KO) did not significantly suppress urinary PGEM and PGIM after cold exposure. A two-way ANOVA showed a significant effect of housing temperature, but not genotype, on urinary PGEM and PGIM. Genotype, temperature, interaction: for PGEM, $p = 0.7436$, $p < 0.0001$, and $p = 0.5985$; and for PGIM, $p = 0.0624$, $p < 0.0001$, and $p = 0.2956$. Holm-Sidak's multiple comparison tests were used to test significant differences between controls and COX-2 KOs at 28°C and 5°C. Data are expressed as mean ± SEM. **$p < 0.01$; ****$p < 0.0001$; n = 8–10.

(E) The capacity for generation of PGI_2 (6-keto-$PGF_{1\alpha}$, the hydrolysis product of PGI_2) and PGE_2 was not significantly increased in iWAT of control and COX-2 KO mice at 5°C, compared with 28°C. A two-way ANOVA showed no significant effect of cold exposure on 6-keto-$PGF_{1\alpha}$ and PGE_2 in iWAT. Data are expressed as mean ± SEM. $p > 0.05$; n = 13–15 (6–7 female and 7–8 male) per genotype.

immediately (Figures S1E–S1G) or after 6 days of exposure of mice to cold (Figures S1H–S1M). The early increase in *Cox-2* mRNA in iBAT from C57BL/6 mice exposed to cold for 1 day (Figure S1G) is of unlikely relevance to thermogenesis, as we observed no changes in body temperature of mice with global depletion of COX-2 during cold exposure (discussed later in Figure 3A). Further, we measured *Cox-2* and *Cox-1* gene expression in mice on a BuB/BnJ background and a 129Sv background to validate our findings and found no increase in any adipose tissue in response to cold exposure (Figures S1N–S1S).

Cold Increases Prostaglandin Biosynthesis in Mouse Heart but Not in Adipose Tissues

Since COX-2 protein was undetected in adipose tissues, and *COX-2* gene expression was very low, we quantified COX-2-derived prostaglandins as a measure of COX-2 activity in adipose tissues. We generated mice with a genetic deletion of COX-2, both universally (COX-2 KO) and specifically in the adipose tissue (Ad-COX2 KO), to test directly the role of COX-2. Additionally, to avoid the multiple developmental consequences of deleting COX-2 conventionally (Morham et al., 1995), we deleted the gene postnatally, using a

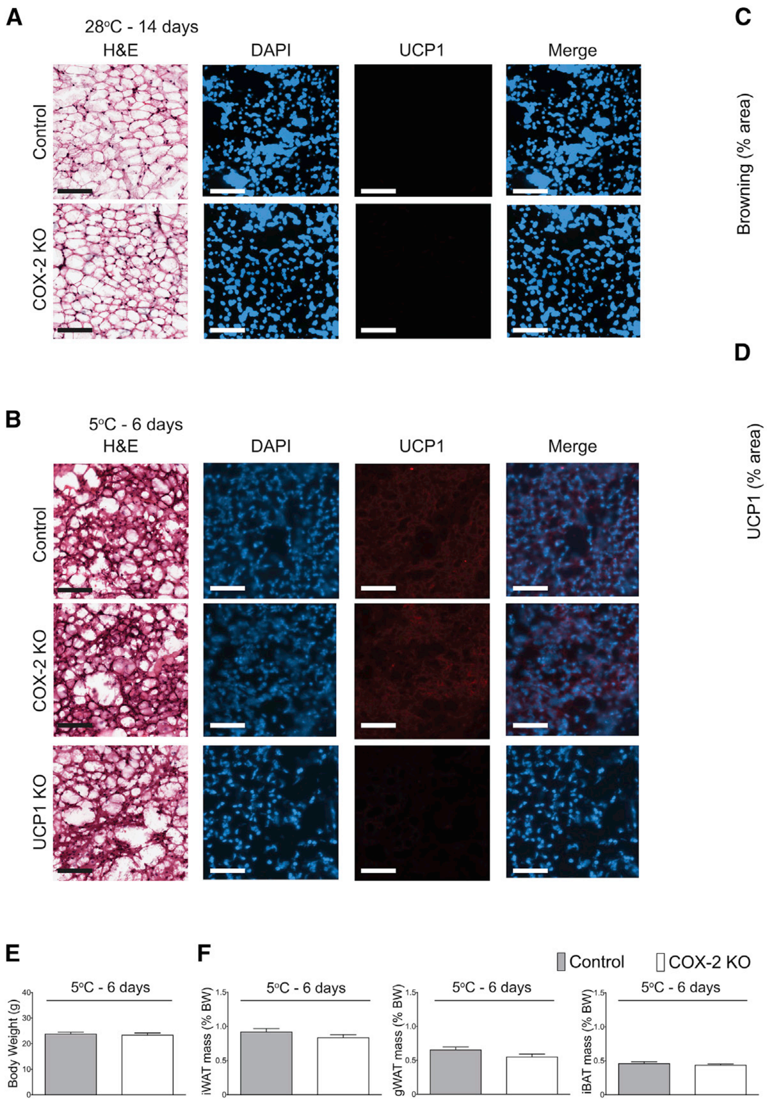

Figure 2. Deletion of COX-2 Fails to Suppress Cold-Induced Browning and UCP1 in Adipose Tissues of Mice

(A and B) H&E staining and immunofluorescence (IF) for the detection of UCP1 in iWAT sections from control and COX-2 KO mice. H&E staining revealed no cells with browning characteristics, and IF did not detect UCP1 in iWAT from mice maintained at thermoneutral conditions (28°C) (A). Cells with browning characteristics and UCP1 were detected in iWAT from mice exposed to cold for 6 days (B). iWAT from UCP1 KO mice was used as a negative control for the immunofluorescent detection of UCP1. Scale bars represent 50 μm.

(C) ImageJ was used to quantify the area containing smaller cells rich in cytoplasmic staining from H&E and expressed as percentage area of the section. A two-way ANOVA revealed no significant difference of brown-like cells between control and COX-2 KO mice after cold exposure (genotype, $p = 0.931$; temperature, $p < 0.0001$; and interaction, $p = 0.9309$). Data are expressed as mean ± SEM. n = 4 per group.

(D) ImageJ was used to quantify IF detecting UCP1 in areas containing smaller cells rich in cytoplasmic staining from H&E. IF is expressed as percentage area of the section. A two-way ANOVA revealed no significant difference of UCP1 detection between control and COX-2 KO mice after cold exposure (genotype, $p = 0.8095$; temperature, $p < 0.0001$; interaction, $p = 0.8095$). Data are expressed as mean ± SEM. n = 4 per group.

(E and F) Deletion of COX-2 fails to alter body weight (E) and mass of adipose tissues (F) of female mice in the cold. A Mann-Whitney test (two-tailed) revealed no significant effect of COX-2 deletion on body weight and mass of adipose tissues (percent body weight, wet weight) of mice after cold exposure, $p > 0.05$. Data are expressed as mean ± SEM. n = 4 per group.

tamoxifen-induced Cre recombinase, treating the mice at 8 weeks of age (Yu et al., 2012). Tamoxifen has been reported to affect the reproductive system in male mice (Taguchi, 1987). In our study, we did not observe abnormal behavior in either control or COX-2 KO mice of both sexes for up to 1 year after tamoxifen administration. Genetic deletion of COX-2 in differentiated adipocytes was accomplished with the use of an adiponectin promoter driving the expression of Cre recombinase (Eguchi et al., 2011). As expected, COX-2 was undetected by western blotting in WAT and BAT of COX-2 KO mice (Figure 1A;

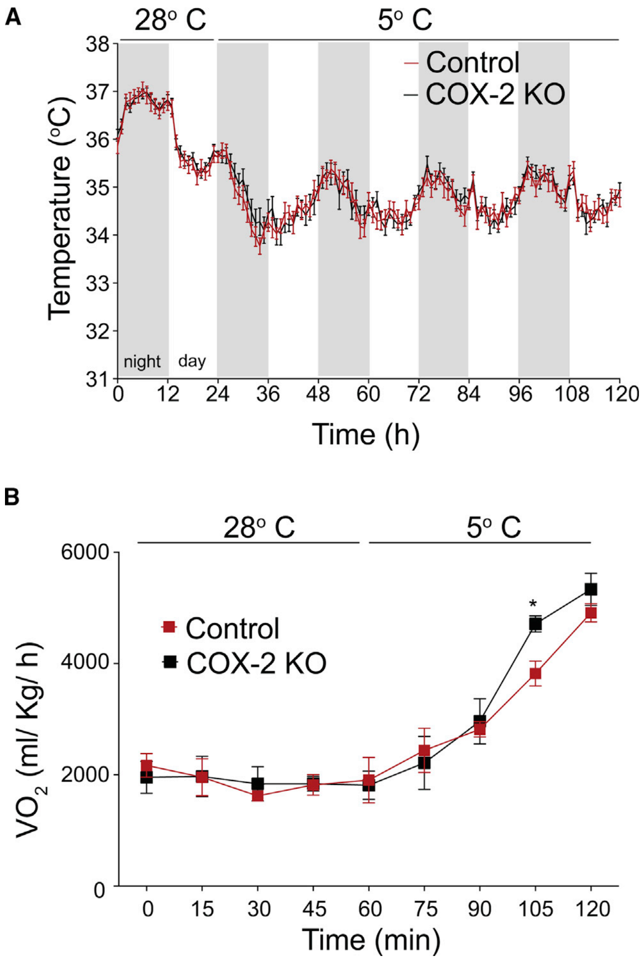

Figure 3. Deletion of COX-2 Fails to Alter Body Temperature and Energy Expenditure of Mice during Cold Exposure

(A) Interscapular temperature in control and COX-2 KO mice. Telemetry transmitters were implanted subcutaneously in the interscapular area of the backs of the mice. Temperatures were recorded after the mice were fully recovered. The mice were acclimatized at 28°C, and then the temperature of the housing incubator was reduced to 5°C at 7 p.m. (lights off). There was no difference in interscapular temperature between control (red line) and COX-2 KO (black line) mice at 28°C and 5°C. Data are expressed as mean ± SEM. n = 12–18 (n = 4 from day 2 at 5°C).

(B) Deletion of COX-2 fails to affect VO_2 of mice housed at 28°C and 5°C. VO_2 increased in mice during cold exposure. A two-way ANOVA revealed a significant effect of temperature, but not of genotype, on VO_2 of mice (genotype, $p = 0.3408$; temperature, $p < 0.0001$; interaction, $p = 0.6510$). Holm-Sidak's multiple comparison tests were used to test significant differences between controls and COX-2 KOs at 28°C and 5°C. Data are expressed as mean ± SEM. n = 4 per group.

Figure S1A). COX-1 in adipose tissues was unaffected by the deletion of COX-2 in mice both at 28°C and after exposure to cold for 6 days (Figure 1B; Figure S1B). *Cox-2* gene expression was reduced in adipose tissues from COX-2 KO mice maintained at 28°C (Figures S2A–S2F). *Cox-1* gene expression in adipose tissues from COX-2 KO mice was unaltered compared to its expression in adipose tissues from control mice (Figures S1H–S1M).

COX-2-derived prostaglandin metabolites in urine increased after exposure of control mice to cold for 6 days, compatible with an increase in COX-2 activity in response to cold (Figure 1C; Figure S1T). Consistent with this possibility, COX-2 KO mice maintained at 28°C have lower levels of COX-2-derived prostaglandin metabolites in urine and show no increase of metabolite excretion in response to cold (Figure 1C; Figure S1T). In contrast, mice lacking COX-2 in adipose tissues alone have no alteration in metabolite excretion under basal conditions and augment their formation in response to cold (Figure 1D; Figure S1U). This indicates that the increase in COX-2 activity in response to cold takes place outside adipose tissues. Further, to support this, we measured COX-2-derived prostaglandins in inguinal adipose tissue from mice exposed to cold for 6 days and found no increase in inguinal adipose tissue prostaglandins in control or COX-2 KO animals (Figure 1E). We did observe a trend toward an increase in prostaglandin concentration in gWAT and iBAT (which reached statistical significance for PGE_2 in iBAT) (Figures S1V and S1W). Since we found no increase in COX-2 or COX-1 in response to cold in these tissues, the changes likely reflect the play of chance or cold-induced lipolysis (Shaw and Ramwell, 1968). We sought other tissues that might respond to the cold challenge, establishing that *COX-2* gene expression was increased in the hearts of mice exposed to cold but in no other tissues that we examined (Figure S1X). This suggests that the heart is at least one source of the systemic increase in prostaglandin biosynthesis reflected to the increased prostaglandin urinary metabolites after cold exposure.

Cold-Induced Browning of iWAT Is Independent of Adipose Tissue COX-2

Having found that COX-2 activity in adipose tissues does not increase in response to cold, we next investigated iWAT browning in response to cold in COX-2 KO mice. Wild-type mice exposed to cold developed browning of iWAT, as reflected by changes in morphology and UCP1 expression (Figures 2A–2D and S2A). UCP1 KO mice (graciously shared by Dr. Lazar) were used to optimize the specificity of UCP1 detection by immunofluorescence using a non-commercially available antibody (Dr. Seale provided the antibody). COX-2 KO mice showed changes in morphology and UCP1 expression in iWAT in response to cold indistinguishable from that in controls (Figures 2A–2D and S2A). The body weight of COX-2 KO mice was not different from that of control mice both before (data not shown) and after cold exposure (Figures 2E and S2B). Similarly, the weights of iWAT, gWAT, and iBAT from COX-2 KO mice exposed to cold were not different from those of controls (Figures 2F and S2B). We then measured body temperature and energy expenditure as physiological outcomes of browning in the adipose tissue in COX-2 KO mice (Figure 3). The body temperature of COX-2 KO mice was not different from that of control mice, both at thermoneutrality and after exposure to cold for 6 days (Figures 3A and S3A). Consistent with this observation, energy expenditure in response to cold was not different in COX-2 KO mice (Figure 3B). To control for the effect of iBAT activation on body temperature and energy expenditure in response to cold, we measured UCP1 in iBAT after cold exposure but found no difference by genotype, suggesting that iBAT activation was not different in COX-2 KO compared to control mice (Figures S3B–S3E). Similarly, deletion of COX-2 did not impede cold-induced increases in thermogenic genes (i.e., *Ucp1*, *Cidea*, and *Cox8b*) (Figures S3F–S3N).

Pharmacological and genetic inactivation of COX-2 has been reported by others to inhibit browning of WATs in mice when placed in a cold environment (Madsen et al., 2010; Vegiopoulos et al., 2010). C57BL/6J male mice treated with the non-specific COX inhibitor indomethacin or conventional COX-2 KOs showed lower rectal temperature in response to cold compared to placebo-treated mice or wild-type (WT) mice in the cold (Madsen et al., 2010). However, using postnatal deletion of COX-2, we failed to detect a significant change in body temperature between our COX-2 KOs and littermate controls. Here, we used a continuous temperature transmitter recording system, implanted subcutaneously, and monitored temperature both during the day and at night, with housing temperatures set at 28°C and 5°C. In addition, deletion of COX-2 did not alter body weight, the mass of adipose tissues, and energy expenditure in mice during cold exposure. The discrepancy with previous results may reflect the residual impact on the postnatal phenotype of COX-2 depletion during embryogenesis in the conventional COX-2 KOs. Similarly, the skin and hair development defects (Neufang et al., 2001) in K5COX-2 mice, which overexpress COX-2 in skin, would be expected to demand increased thermogenesis to maintain body temperature (Nedergaard and Cannon, 2014). Aside from these limitations, the physiological relevance of an undocumented but presumably substantially augmented (Bol et al., 2002) and sustained increase in prostaglandin biosynthesis in COX-2 overexpressing mice is, at best, arguable. Similar constraints apply to the reports that micromolar concentrations of carbaprostacyclin, a synthetic analog of the COX-2 product, prostacyclin, promote browning of adipocytes in *in vitro* cell-culture models (Bayindir et al., 2015; Ghandour et al., 2016). Endogenous prostanoids, such as prostacyclin, are formed transiently and, at femtomolar to picomolar quantities, to act locally (FitzGerald et al., 1981).

Despite activation of thermogenesis, we did not detect a significant increase in *COX-2* mRNA expression in all three adipose tissues from our mouse strains. COX-2 protein was also not detected in control and COX-2 KO mice before and after cold exposure. Deletion of COX-2 in C57BL/6 mice did not impede the cold-induced increase in UCP1 protein. This is in agreement with the findings of the study published by Madsen et al. (2010), showing COX2-independent UCP1 activity of iBAT in Sv129 mice. Although COX-2 modulates early differentiation and commitment of skeletal muscle precursor cells to brown pre-adipocytes (Sharma et al., 2014), our data are consistent with the hypothesis that COX-2 lacks a physiological role in adipose tissues of mice undergoing thermogenesis in a cold environment.

In summary, cold-induced thermogenesis in iWAT, gWAT, and iBAT of mice is independent of COX-2. Nonetheless, cold-induced cutaneous vasoconstriction coincided with an increase in COX-2 expression in the heart; and systemic prostaglandin biosynthesis, as reflected by urinary PGIM (2,3-dinor 6-keto $PGF_{1\alpha}$) and PGEM (7-hydroxy-5,11-diketotetranorprostane-1,16-dioic acid), is increased, perhaps to counteract the consequences of vasoconstriction to conserve heat loss (Morrison and Nakamura, 2011). The physiological relevance of COX-2 upregulation in the heart after cold exposure warrants further investigation.

EXPERIMENTAL PROCEDURES

Animals

The postnatal global COX-2 KOs and COX2 flox/flox mice (as their littermate WT controls) used in this study were generated as described previously (Wang et al., 2009). Briefly, mice with Cre-ER (estrogen receptor) (Hayashi and McMahon, 2002) that render Cre activity inducible by tamoxifen were crossed with COX-2 flox/flox mice to generate the COX-2 KO mice. Both KOs and WT controls at 8 weeks old were given tamoxifen (intraperitoneally [i.p.], 100 mg/kg of body weight per day) for 5 consecutive days to delete COX-2. All experiments were performed 1 month after the last day's tamoxifen injection, when the possibility of residual drug effects was minimized. Control, COX-2 KO, and adipocyte-specific COX-2 KOs (Ad-COX-2 KO, adiponectin-Cre; Eguchi et al., 2011) were on C57BL/6 backgrounds. UCP1 KO animals were provided by Dr. Lazar. C57BL/6 mice were purchased from Jackson Laboratory. Most results from female mice are presented in the Results and Discussion section here, and results from male mice are presented in the Supplemental Information. All animals in this study were housed according to the guidelines of the Institutional Animal Care and Use Committee (IACUC) of the University of Pennsylvania. All experimental protocols were approved by the IACUC.

Measurement of Body Temperature

Mice were anesthetized using a solution containing ketamine, xylazine, and acepromazine. The dorsal area of mice was shaved to remove hair, and a horizontal incision was made for insertion of a telemetry transmitter (Data Sciences International).

Cold-Exposure Experiments

Different strains of mice at 12–16 weeks old were individually housed during acclimatization at 28°C for 14 days in a ventilated temperature incubator. After acclimatization, the temperature of the incubator was switched to 5°C to expose the animals to this temperature for 1 or 6 days. It took less than 10 min for the incubator temperature to drop from 28°C to 5°C. For 129Sv mice, animals were acclimatized at 28°C for 6 days, followed by 6 days at 5°C (Madsen et al., 2010). Animals in the incubator were exposed to a normal 12-hr:12-hr light:dark cycle and had free access to food pellets and water.

Mass Spectrometric Analysis of Prostanoids

Urinary prostanoid metabolites were measured by liquid chromatography/mass spectrometry as described previously (Song et al., 2007). Such measurements provide a noninvasive, time-integrated measurement of systemic prostanoid biosynthesis. The capacity of adipose depots to form prostaglandins was estimated by measuring PGE_2 and the hydrolysis product of PGI_2, 6-keto $PGF_{1\alpha}$. Details of the method can be found in the Supplemental Experimental Procedures.

Quantification of Cyclooxygenase Protein by Mass Spectrometry

The precise relative expression of cyclooxygenase isoforms was measured using nano-spray liquid chromatography/multiple reaction monitoring (LC-MRM) mass spectrometry (Li et al., 2014). Details of the method can be found in the Supplemental Experimental Procedures.

Immunofluorescent Detection of UCP1

Fresh frozen tissue slides from iWAT were stained for UCP1 immunofluorescence and H&E. A non-commercially available antibody against UCP1 was used for the immunofluorescent detection (produced by AstraZeneca and gracefully shared by Dr. Seale). Details can be found in the Supplemental Experimental Procedures.

Statistical Analysis

Most analyses were tested using two-way ANOVA (genotype and temperature factors). The Holm-Sidak's post-test was used to compare the differences between the means only if the ANOVA indicated significance at $p < 0.05$. A Mann-Whitney (two-tailed, temperature factor, 2 groups) test was also used where appropriate. Separate conclusions were drawn for male and female mice. Sample sizes were based on variability of the test measurement and the desire to detect a minimal 10% difference in the variables assessed with $\alpha = 0.05$ and power $(1 - \beta) = 0.8$.

SUPPLEMENTAL INFORMATION

Supplemental Information includes Supplemental Experimental Procedures and three figures and can be found with this article online at https://doi.org/10.1016/j.celrep.2018.06.082.

ACKNOWLEDGMENTS

We gratefully acknowledge the technical support of Helen Zou and Wenxuan Li-Feng. We want to thank Dr. Lazar for providing us the UCP1 KO mice. We also thank Dr. Seale for providing us with the antibody for the immunofluorescent detection of UCP1. This work was supported by grants from the NIH (P01 HL062250 and 1U54 HL117798). G.A.F. is the McNeil Professor of Translational Medicine and Therapeutics.

AUTHOR CONTRIBUTIONS

S.Y.T., G.K.P., and G.A.F. conceived of the study, designed and/or performed the experiments, analyzed the data, and wrote and/or edited the manuscript; X.L. was responsible for quantification of COX protein by mass spectrometry; K.N.T. assisted with mouse experiments; I.V. and D.L. assisted with immunofluorescence; W.Y. contributed to rt-qPCR experiments; L.H. contributed to HE experiment and data analysis; and J.L. contributed to prostanoid analysis.

DECLARATION OF INTERESTS

The authors declare no competing interests.

Received: March 17, 2016
Revised: April 30, 2018
Accepted: June 19, 2018
Published: July 24, 2018

REFERENCES

Bayindir, I., Babaeikelishomi, R., Kocanova, S., Sousa, I.S., Lerch, S., Hardt, O., Wild, S., Bosio, A., Bystricky, K., Herzig, S., and Vegiopoulos, A. (2015). Transcriptional pathways in cPGI2-induced adipocyte progenitor activation for browning. Front. Endocrinol. (Lausanne) *6*, 129.

Bol, D.K., Rowley, R.B., Ho, C.P., Pilz, B., Dell, J., Swerdel, M., Kiguchi, K., Muga, S., Klein, R., and Fischer, S.M. (2002). Cyclooxygenase-2 overexpression in the skin of transgenic mice results in suppression of tumor development. Cancer Res. *62*, 2516–2521.

Eguchi, J., Wang, X., Yu, S., Kershaw, E.E., Chiu, P.C., Dushay, J., Estall, J.L., Klein, U., Maratos-Flier, E., and Rosen, E.D. (2011). Transcriptional control of adipose lipid handling by IRF4. Cell Metab. *13*, 249–259.

FitzGerald, G.A., Brash, A.R., Falardeau, P., and Oates, J.A. (1981). Estimated rate of prostacyclin secretion into the circulation of normal man. J. Clin. Invest. *68*, 1272–1276.

Ghandour, R.A., Giroud, M., Vegiopoulos, A., Herzig, S., Ailhaud, G., Amri, E.Z., and Pisani, D.F. (2016). IP-receptor and PPARs trigger the conversion of human white to brite adipocyte induced by carbaprostacyclin. Biochim. Biophys. Acta *1861*, 285–293.

Hayashi, S., and McMahon, A.P. (2002). Efficient recombination in diverse tissues by a tamoxifen-inducible form of Cre: a tool for temporally regulated gene activation/inactivation in the mouse. Dev. Biol. *244*, 305–318.

Li, X., Fries, S., Li, R., Lawson, J.A., Propert, K.J., Diamond, S.L., Blair, I.A., FitzGerald, G.A., and Grosser, T. (2014). Differential impairment of aspirin-dependent platelet cyclooxygenase acetylation by nonsteroidal antiinflammatory drugs. Proc. Natl. Acad. Sci. USA *111*, 16830–16835.

Madsen, L., Pedersen, L.M., Lillefosse, H.H., Fjaere, E., Bronstad, I., Hao, Q., Petersen, R.K., Hallenborg, P., Ma, T., De Matteis, R., et al. (2010). UCP1 induction during recruitment of brown adipocytes in white adipose tissue is dependent on cyclooxygenase activity. PLoS ONE *5*, e11391.

Morham, S.G., Langenbach, R., Loftin, C.D., Tiano, H.F., Vouloumanos, N., Jennette, J.C., Mahler, J.F., Kluckman, K.D., Ledford, A., Lee, C.A., and Smithies, O. (1995). Prostaglandin synthase 2 gene disruption causes severe renal pathology in the mouse. Cell *83*, 473–482.

Morrison, S.F., and Nakamura, K. (2011). Central neural pathways for thermoregulation. Front. Biosci. *16*, 74–104.

Nedergaard, J., and Cannon, B. (2014). The browning of white adipose tissue: some burning issues. Cell Metab. *20*, 396–407.

Neufang, G., Furstenberger, G., Heidt, M., Marks, F., and Müller-Decker, K. (2001). Abnormal differentiation of epidermis in transgenic mice constitutively expressing cyclooxygenase-2 in skin. Proc. Natl. Acad. Sci. USA *98*, 7629–7634.

Sharma, A., Huard, C., Vernochet, C., Ziemek, D., Knowlton, K.M., Tyminski, E., Paradis, T., Zhang, Y., Jones, J.E., von Schack, D., et al. (2014). Brown fat determination and development from muscle precursor cells by novel action of bone morphogenetic protein 6. PLoS One *9*, e92608.

Shaw, J.E., and Ramwell, P.W. (1968). Release of prostaglandin from rat epididymal fat pad on nervous and hormonal stimulation. J. Biol. Chem. *243*, 1498–1503.

Smith, W.L. (1992). Prostanoid biosynthesis and mechanisms of action. Am. J. Physiol. *263*, F181–F191.

Song, W.L., Lawson, J.A., Wang, M., Zou, H., and FitzGerald, G.A. (2007). Noninvasive assessment of the role of cyclooxygenases in cardiovascular health: a detailed HPLC/MS/MS method. Methods Enzymol. *433*, 51–72.

Taguchi, O. (1987). Reproductive tract lesions in male mice treated neonatally with tamoxifen. Biol. Reprod. *37*, 113–116.

Vegiopoulos, A., Müller-Decker, K., Strzoda, D., Schmitt, I., Chichelnitskiy, E., Ostertag, A., Berriel Diaz, M., Rozman, J., Hrabe de Angelis, M., Nüsing, R.M., et al. (2010). Cyclooxygenase-2 controls energy homeostasis in mice by de novo recruitment of brown adipocytes. Science *328*, 1158–1161.

Wang, D., Patel, V.V., Ricciotti, E., Zhou, R., Levin, M.D., Gao, E., Yu, Z., Ferrari, V.A., Lu, M.M., Xu, J., et al. (2009). Cardiomyocyte cyclooxygenase-2 influences cardiac rhythm and function. Proc. Natl. Acad. Sci. USA *106*, 7548–7552.

Yu, Z., Crichton, I., Tang, S.Y., Hui, Y., Ricciotti, E., Levin, M.D., Lawson, J.A., Puré, E., and FitzGerald, G.A. (2012). Disruption of the 5-lipoxygenase pathway attenuates atherogenesis consequent to COX-2 deletion in mice. Proc. Natl. Acad. Sci. USA *109*, 6727–6732.

Cell Reports, Volume *24*

Supplemental Information

Cold-Induced Browning of Inguinal White Adipose Tissue Is Independent of Adipose Tissue Cyclooxygenase-2

Georgios K. Paschos, Soon Yew Tang, Katherine N. Theken, Xuanwen Li, Ioannis Verginadis, Damien Lekkas, Lindsay Herman, Weili Yan, John Lawson, and Garret A. FitzGerald

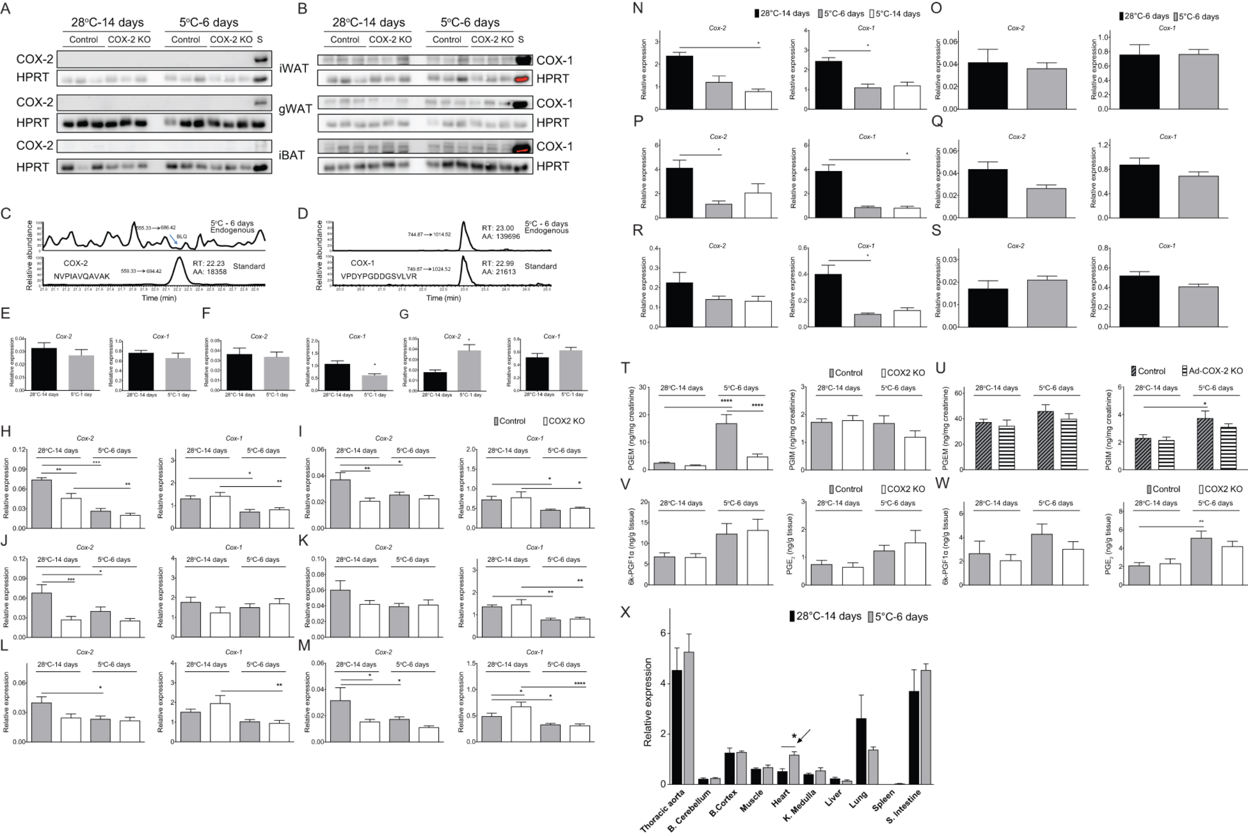
A
28°C-14 days
5°C-6 days
Control
COX-2 KO
S
COX-2
HPRT
iWAT
gWAT
iBAT
B
COX-1
C
5°C - 6 days Endogenous
COX-2
NVPIAVQAVAK
RT: 22.23
AA: 18358
Standard
Relative abundance
Time (min)
D
COX-1
VPDYPGDDGSVLVR
RT: 23.00
AA: 139696
RT: 22.99
AA: 21613
E
F
G
Cox-2
Cox-1
Relative expression
28°C-14 days
5°C-1 day
H
I
J
K
L
M
Control
COX2 KO
N
O
P
Q
R
S
28°C-14 days
5°C-6 days
5°C-14 days
28°C-6 days
T
U
V
W
PGEM (ng/mg creatinine)
PGIM (ng/mg creatinine)
Ad-COX-2 KO
6k-PGF1α (ng/g tissue)
PGE2 (ng/g tissue)
X
Thoracic aorta
B. Cerebellum
B.Cortex
Muscle
Heart
K. Medulla
Liver
Lung
Spleen
S. Intestine

Figure S1. Cold Exposure Fails to Upregulate COX-2 and COX-1 Protein Levels or gene expression in Adipose Tissues of Mice, related to Figure 1

(A, B) COX-2 (A) and COX-1 (B) protein levels were examined by immunoblotting in inguinal white adipose tissue (iWAT), gonadal white adipose tissue (gWAT) and interscapular brown adipose tissue (iBAT) from male mice housed at 28°C and 5°C. COX-2 (A) was not detected in adipose tissues regardless of genotypes and housing temperatures. COX-1 levels (B) were not influenced in the adipose tissues by genotype or housing temperatures. HPRT was used as a loading control. Representative images of 6-8 independent experiments are shown. S- spleen as positive control.

(C, D) The relative abundance of COX-2 and COX-1 in adipose tissue was measured by isotope dilution mass spectrometry as descripted in the Supplemental Experimental Procedures. A typical spectrum of COX-2 (C) and COX-1 (D) protein extracted from adipose tissue (iWAT) is shown. The peak area (AA) of the unique proteotypic peptides detected by the mass spectrometry was used to quantify the endogenous expression of its protein by comparing to the spiked internal standard peptides, which eluted at the same retention time (RT) in liquid chromatography. BLQ: below limit of quantification. Limit of quantification is < fmol, COX-2 standard peptides- NVPIAVQAVAK, COX-1 standard peptides- VPDYPGDDGSVLVR.

(E-G) *COX-2* and *COX-1* expression relative to *Hprt* in iWAT (E), gWAT (F) and iBAT (G) from mice housed at 28°C for 14 days and at 5°C for 1 day. *COX-2* and *COX-1* transcripts were examined by quantitative real-time PCR as described in the Supplemental Experimental Procedures. *COX-2* expression in iBAT increased in C57BL/6 male mice housed at 5°C for 1 day. Mann-Whitney tests (2-tailed) revealed significant increase in *COX-2* in iBAT and decrease in *COX-1* in gWAT after cold exposure. Data are expressed as mean±SEMs. *$p < 0.05$; n=4-11 per group.

(H-M) *Cox-2* and *Cox-1* expression relative to *Hprt* in iWAT (H, I), gWAT (J, K) and iBAT (L, M) from male (H, J, L) and female (I, K, M) COX-2 KO and control mice housed at 28°C for 14 days and at 5°C for 6 days. Two-way ANOVA showed a significant effect of cold exposure on *Cox-2* and *Cox-1* transcript levels in various adipose tissues (genotype, temperature, interaction). Holm-Sidak's multiple comparison tests were used to test significant differences between Control and COX-2 KOs at 28°C and 5°C. Data are represented as mean±SEMs. *$p < 0.05$, **$p < 0.01$, ***$p < 0.001$, ****$p < 0.0001$; (H, J, L) n=5-11 (I, K, M) n=8-16 per genotype.

(N-R) *Cox-2* and *Cox-1* expression relative to *Hprt* in iWAT (N), gWAT (P) and iBAT (R) from female BuB/BnJ mice housed at 28°C for 14 days and at 5°C for 6 and 14 days. One-way ANOVA (Kruskal-Wallis test) showed significant decreases in COX-2 and COX-1 in different adipose tissue depots after cold exposure. Data are represented as mean±SEMs. *$p < 0.05$; n=4 per group.

(O-S) *Cox-2* and *Cox-1* expression relative to *Hprt* in iWAT (O), gWAT (Q) and iBAT (S) from male 129Sv mice housed at 28°C for 14 days and at 5°C for 6 days. 2-tailed Mann-Whitney tests showed no significant changes. Data are represented as mean±SEMs. $p > 0.05$; n=4-6 per group.

(T) Urine samples were collected from mice housed at 28°C and 5°C, and prostanoids metabolites were analyzed by liquid chromatography/ mass spectrometry as described in the Supplemental Experimental Procedures.

Urinary 7-hydroxy-5, 11-diketotetranorprostane-1, 16-dioic acid (PGEM) but not 2, 3-dinor 6-keto $PGF_{1\alpha}$ (PGIM) was increased in control mice at 5°C for 6 days compared with 28°C. Global COX-2 deletion depressed urinary PGEM. Two-way ANOVA showed a significant effect of cold exposure and genotype on urinary PGEM. Holm-Sidak's multiple comparison tests were used to test significant differences between controls and COX-2 mutants at 28°C and 5°C. Data are represented as mean±SEMs. *$p < 0.05$, **$p < 0.01$; n=7-9.

(U) Disruption of COX-2 in adipocytes (Ad-COX2 KO) did not significantly suppress urinary PGEM and PGIM after cold exposure in male mice. Two-way ANOVA showed a significant effect of housing temperature but not genotype on urinary PGIM. Holm-Sidak's multiple comparison tests were used to test significant differences between Controls and Ad-COX2 KOs at 28°C and 5°C. Data are represented as mean±SEMs. *$p < 0.05$, n=9-10).

(V and W) The capacity for generation of PGI_2 (6-keto-$PGF_{1\alpha}$, the hydrolysis product of PGI_2) and PGE_2 were not significantly increased in gWAT (V) from control and COX-2 KO mice housed at 5°C compared with mice housed at 28°C, except for PGE_2 in iBAT (W). Two-way ANOVA showed a significant effect of cold-exposure on PGE_2 in iBAT. Holm-Sidak's multiple comparison tests were used to test significant differences between control and COX-2 KOs housed at 28°C and 5°C. Data are represented as mean±SEMs. **$p < 0.01$; n=13-15 (6-7 female and 7-8 male) per genotype.

(X) *Cox-2* expression relative to *Hprt* in various tissues from control mice housed at 28°C for 14 days and 5°C for 6 days. *Cox-2* transcripts were examined by quantitative real-time PCR as described in the Supplemental Experimental Procedures. A Mann-Whitney test (2-tailed) revealed a significant effect of housing temperature on *Cox-2* expression in heart tissue. Data are expressed as mean±SEMs. $p < 0.05$; n=4-5.

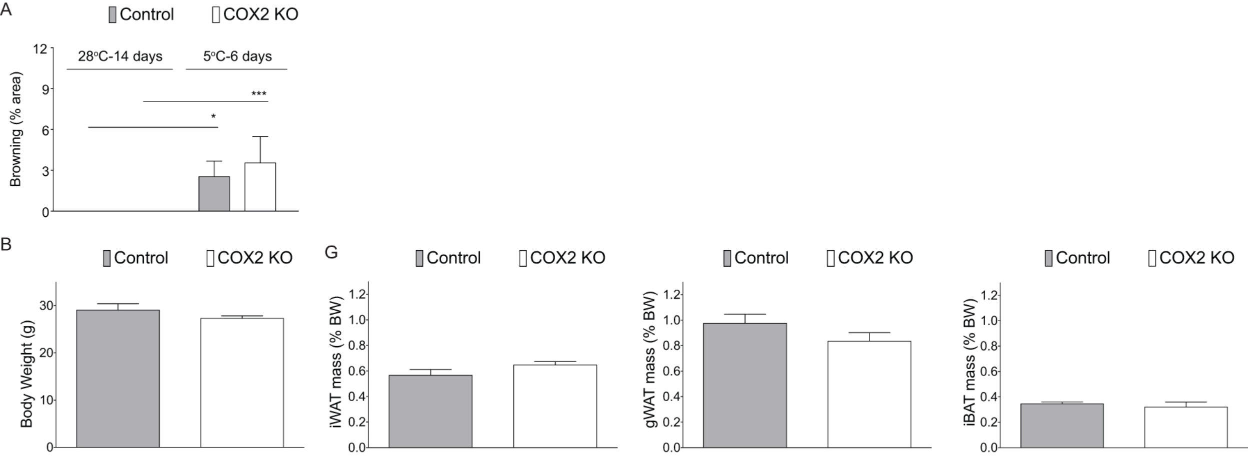

A
Control
COX2 KO
28°C-14 days
5°C-6 days
Browning (% area)
12
9
6
3
0
***
*
B
Control
COX2 KO
Body Weight (g)
30
20
10
0
G
Control
COX2 KO
iWAT mass (% BW)
Control
COX2 KO
gWAT mass (% BW)
Control
COX2 KO
iBAT mass (% BW)
1.2
1.0
0.8
0.6
0.4
0.2
0.0

Figure S2. H&E Staining Quantification, Body, Tissue Weight of COX-2 KO Mice, related to Figure 2

(A) Hematoxylin/Eosin (H&E)-staining in iWAT sections from control and COX-2 KO mice was used to quantify the area containing smaller cells rich in cytoplasmic staining as a measure of browning. Two-way ANOVA revealed no significant difference of brown-like cells between control and COX-2 KO mice after cold exposure (genotype, $p=0.3202$; temperature, $p<0.0001$; interaction, $p=0.3202$).
(B) Deletion of COX-2 fails to alter body weight and mass of iWAT, gWAT and iBAT (% of body weight (BW)) of male mice housed at 5°C for 6 days. A Mann-Whitney test (2-tailed) revealed no significant effect of COX-2 deletion on body weight and mass of adipose tissues (% body weight, wet weight) of mice after cold exposure, $p>0.05$. Data are expressed as mean±SEMs. n=3-4 per group.

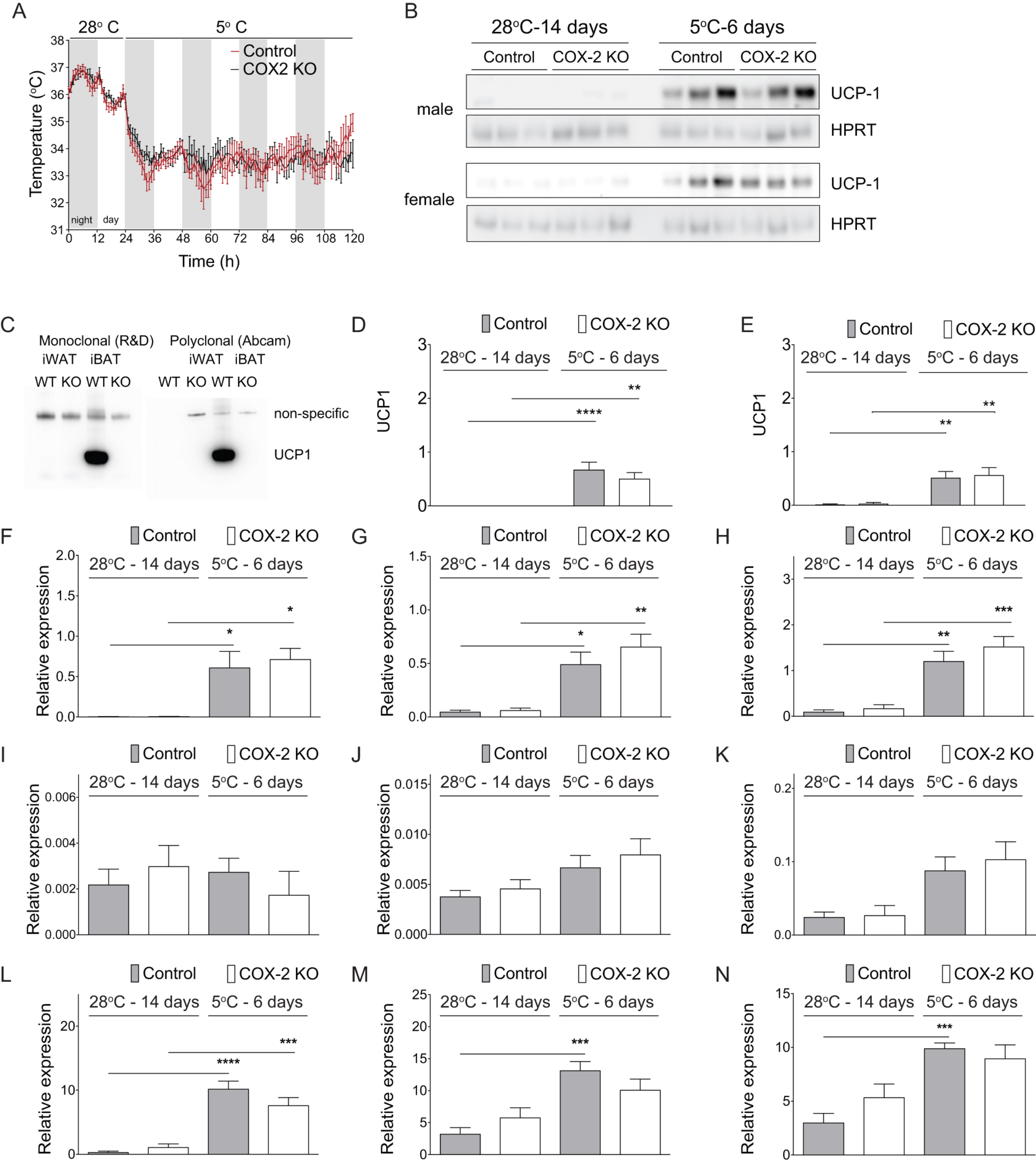
A
28° C
5° C
Control
COX2 KO
Temperature (°C)
night
day
Time (h)
B
28°C-14 days
5°C-6 days
Control
COX-2 KO
male
female
UCP-1
HPRT
C
Monoclonal (R&D)
Polyclonal (Abcam)
iWAT iBAT
WT KO WT KO
non-specific
UCP1
D
E
F
G
H
I
J
K
L
M
N
Control
COX-2 KO
28°C - 14 days
5°C - 6 days
UCP1
Relative expression

Figure S3. Deletion of COX-2 Fails to Alter Body Temperature and COX-2 Protein, Gene Expression during Cold Exposure, related to Figure 3

(A) Interscapular temperature in control and COX-2 KO female mice. Telemetry transmitters were implanted subcutaneously in the interscapular area of the backs of the mice. Temperatures were recorded after the mice were fully recovered. The mice were acclimatized at 28°C and then the temperature of the housing incubator was reduced to 5°C at 7pm (lights off). There was no difference in interscapular temperature between control (red line) and COX-2 KO (black line) mice at 28°C and 5°C. Data are expressed as mean±SEMs. n=13.

(B) UCP1 protein levels were examined by immunoblotting in iBAT from mice housed at 28°C and 5°C. UCP1 was up-regulated in iBAT after cold exposure. Representative images from 8 independent immunoblotting studies are shown. HPRT was used as a loading control.

(C) Immunoblotting for UCP1 using polyclonal #ab10983 antibody from Abcam and monoclonal # 535436 antibody from R&D in iWAT and iBAT from wild-type and UCP1 KO mice housed at 5°C for 6 days was used to determine the specificity of detection. UCP1 was not detected in iWAT from either wild-type or KO mice. UCP1 was detected in iBAT from wild-type mice but not from UCP1 KO mice indicating the specificity of the detection.

(D, E) ImageJ was used to quantify band intensity from immunoblots in Supplemental Figure 4B for male (D) and female (E) mice. Two-way ANOVA showed no significant difference in UCP1 expression between control and COX-2 KO after cold exposure (male- genotype, temperature, interaction p=0.3487, p<0.0001, p=0.3487; female, p=0.7240, p<0.0001, p=0.8581). Data are represented as mean (min to max). n=8 per group.

(F-N) *Ucp-1* (F, I, L), *Cidea* (G, J, M), and *Cox8b* (H, K, N), expression relative to *Hprt* in iWAT (F, G, H), gWAT (I, J, K) and iBAT (L, M, N) from COX-2 KO and control mice housed at 28°C for 14 days and at 5°C for 6 days. Mann-Whitney tests (2-tailed) revealed significant increases in *Ucp-1, Cidea,* and *Cox8b* expression in different adipose tissue depots after cold exposure. Data are represented as mean±SEMs. *p< 0.05, **p< 0.01; n=4-6 per group.

Supplemental Experimental Procedures

Preparation of Mouse Tissues for Quantitative Real-Time PCR Analysis of Gene Expression

Various tissues of mice were harvested after exposure to 28ºC or 5ºC for different days. RNA was extracted using TRIzol® Reagent and RNeasy Kit following the manufacturer's protocol. The concentration and quality of extracted RNA from various tissues were measured using NanoDrop® 1000 (Thermo Scientific, Wilmington, DE) and reverse-transcribed into cDNA using Taqman Reverse Transcription Reagents (Applied Biosystems, Foster City, CA). Quantitative real time PCR was performed using Taqman Gene Expression Assays for COX-1 (cyclooxygenase-1, Mm00477214_m1) and COX-2 (cyclooxygenase-2, Mm00478374_m1) using the ViiA^{TM} 7 real-time PCR system in a 384 well plate. Results were normalized with HPRT (hypoxanthine guanine phosphoribosyl transferase, Mm01545399_m1).

Mass Spectrometric Analysis of Prostanoids

Briefly, mouse urine samples were collected using metabolic cages over a 6 hour period (8am to 2pm). Systemic production of PGI_2 and PGE_2 were determined by quantifying their major urinary metabolites, 2, 3-dinor 6-keto $PGF_{1\alpha}$ (PGIM) and 7-hydroxy-5, 11-diketotetranorprostane-1, 16-dioic acid (PGEM), respectively. Results were normalized with creatinine.

Adipose tissues (inguinal and gonadal WAT and interscapular BAT) were collected from mice housed at 28°C for 14 days and 5°C for 6 days in tubes containing phosphate buffered solution (PBS) and indomethacin (10μM). Adipose tissues were broken up to release prostaglandins into PBS by shaking at high speed with metal beads in a TissueLyser. Samples were then centrifuged at 20,000 x g for 10min at 4°C. Clear supernatant was transferred into a new tube and kept frozen at -80°C until analyses. The capacity of adipose depots to form prostaglandins was estimated by measuring PGE_2 and the hydrolysis product of PGI_2. Results were normalized with tissue weight.

Quantification of Cyclooxygenase Protein by Mass Spectrometry

Whole heart protein lysate was run on SDS-PAGE with COX-1 electrophoresis standard as control. After staining with coomassie Brilliant Blue G-250, gel bands corresponding to COX proteins were excised. This was followed by destaining, reduction and alkylation steps as described in (Li et al., 2009). Stable isotope labeled internal standards for unique proteolytic peptides from both mouse COX-1 (VPDYPGDDGSVLVR) and COX-2 (NVPIAVQAVAK) were spiked into the samples before the samples were digested with trypsin overnight. LC-MRM analysis was performed on a TSQ Vantage triple stage quadrupole mass spectrometer interfaced with a Nano-ACQUITY UPLC system as described in (Wehr et al., 2012). Three unique transitions were monitored for each peptide, and the strongest transition was used for precise relative quantification for each peptide. Quantification was determined from the peak areas of the transitions using Xcalibur QuanBrowser. The relative expressions of COX-1 and COX-2 proteins were calculated using the ratio of peak area of the endogenous peptides to corresponding internal standard.

Energy Expenditure- Oxymax/ Comprehensive Lab Animal Monitoring System (CLAMS)

CLAMS was used to quantitate oxygen consumption (VO_2) of mice during their housing at 28°C and 5°C.

Western Blotting Analysis

Tissue samples were homogenized in RIPA buffer. Protein concentrations of the supernatants were determined with the DC Protein Assay Kit, and 10-20 μg protein in the loading dye was heated before loading onto a 4-12% SDS-PAGE gel for immunoblotting. Separated proteins were transferred to nitrocellulose membranes and probed with antibodies after membrane blocking with non-fat milk (5% in Tris buffer containing 0.05% Tween 20, 1 h) against COX-1 and COX-2 (#160109 and #160106, Cayman Chemical, 1:1000), UCP1 (polyclonal, #ab10983, abcam, 1:1000; monoclonal mouse IgG_{2B} Clone # 535436, R&D, 1:1000) and HPRT (#20975, Santa Cruz Biotechnology, 1:1000). Detection was performed by enhanced chemiluminescence and visualized using the ImageQuant LAS 4000. Band intensity was quantified using ImageJ software and normalized with HPRT. Some blots were first probed with COX-2 antibody, removed with stripping buffer and re-probed with COX-1 antibody.

Immunofluorescent detection of UCP1

Frozen cryosectioned slides of iWAT (12-15 uM) were dried at room temperature for twenty minutes prior to rehydration in PBS with 0.025% TritonX (PBS-T). Samples were blocked with 10% horse serum in PBS-T for thirty minutes at room temperature. UCP1 primary antibody (non-commercially available, Astra Zeneca, shared by Dr. Seale, 1:500 dilution) was added directly to each sample slide and left to incubate overnight at 4C. After washing with PBS-T, samples were incubated with the Northern Lights Alexa 635 secondary antibody in a 1:1000 dilution of incubation buffer for 1 hour at room temperature. Subsequent to another wash step, ~300 uL DAPI counterstain was added to the samples in a 1:2000 dilution with incubation buffer and incubated for five minutes at room temperature. After a final wash, tissues were dried and mounted with VectaShield mounting medium. Stained slides were digitally scanned at 10x magnification on a Zeiss Observer.Z1 microscope. ImageJ was used to quantify stained cells in areas containing smaller cells rich in cytoplasmic staining from H&E and expressed as % area of the entire section.

Supplemental References

Li, X., Xie, C., Jin, Q., Liu, M., He, Q., Cao, R., Lin, Y., Li, J., Li, Y., Chen, P., et al. (2009). Proteomic screen for multiprotein complexes in synaptic plasma membrane from rat hippocampus by blue native gel electrophoresis and tandem mass spectrometry. J Proteome Res *8*, 3475-3486.

Wehr, A.Y., Hwang, W.T., Blair, I.A., and Yu, K.H. (2012). Relative quantification of serum proteins from pancreatic ductal adenocarcinoma patients by stable isotope dilution liquid chromatography-mass spectrometry. J Proteome Res *11*, 1749-1758.